

Free flux flow and the resistive transition in the mixed state of a superconductor

Milind N. Kunchur* and Manlai Liang

Department of Physics and Astronomy, University of South Carolina, Columbia, SC 29208

Jiong Hua and Zhili Xiao

*Material Science Division, Argonne National Laboratory, Argonne, IL 60439 and
Department of Physics, Northern Illinois University, De Kalb, IL 60115*

(Dated: February 26, 2019)

We observed free flux flow (FFF) in Molybdenum-Germanium (MoGe) superconducting films under the most ideal conditions where the response is perfectly Ohmic even in the limit of vanishing electric current and magnetic field. This provided the first opportunity to test in detail fundamental theories of vortex dissipation in the intrinsic pinning-free limit, and to experimentally establish the true dynamics of FFF. The observations are well explained by a heuristic model that includes magnetic pair breaking but do not support the Larkin-Ovchinnikov theory.

PACS numbers: 74.25.Sv, 74.25.Wx, 74.25.Uv, 74.25.Op, 74.25.F-

Keywords: Flux, vortex, vortices, fluxon, Larkin, Ovchinnikov, flow, upper critical field

I. INTRODUCTION AND BACKGROUND

The motion of magnetic flux vortices in the mixed state of type II superconductors is one of the most studied aspects of superconductors. The most fundamental transport regime of the mixed state is the state of free flux flow (FFF) where the “Lorentz” force on the vortices is balanced only by the intrinsic viscous drag, without any additional interactions arising from pinning, elastic strains, thermal gradients, etc. The most basic theories of flux dynamics—starting with the earliest models such as the ones by Bardeen-Stephen¹, Clem², and Tinkham³, through the more recent work of Larkin and Ovchinnikov⁴, and of Troy and Dorsey⁵—address this FFF state. It is thus imperative to experimentally investigate FFF in detail, to elucidate the dynamics and mechanisms of dissipation, and to check the validity of the theories. Surprisingly, this has not been done before; FFF is normally obscured by pinning, which can only be overcome by extraordinarily high values of the current density j and temperature T that approach their critical values. One of the most rudimentary characteristics expected of the FFF regime (as long as j is not large enough to alter the superconducting state), is that the transport response be Ohmic, so that the flux-flow chordal resistivity $\rho_f = E/j$ —not just the differential resistivity $\rho_d = dE/dj$ —is constant. The constancy of $\rho_f(j)$ has not been tested in a sensitive manner before: Previous reports^{6–10} either plot ρ_d (instead of ρ_f) and/or use a logarithmic scale so that the deviation from Ohmic behavior is less conspicuous. In some of these cases^{6–9}, high current densities were able to largely overcome pinning so that ρ became only roughly constant. Nevertheless these previous works were able to at least establish, on a rough overall scale, the adherence to the basic Bardeen-Stephen relation $\rho_f \sim \rho_n B/H_{c2}$, where ρ_n is the normal-state resistivity, B is the magnetic field, and H_{c2} is the upper critical field (we set $\mu_0 = 1$ and use units of Tesla for both the magnetic field B as well as the magnetizing

field H).

A Molybdenum-Germanium (MoGe) superconducting film is an ideal system to explore the fundamentals of vortex dynamics at their most basic level for the following reasons:

- (1) MoGe is isotropic and does not have the complication of layers. Its high disorder takes it well into the dirty limit and high- κ limit. Furthermore MoGe is a classic weak-coupling BCS superconductor with a gap-to-critical-temperature ratio $\Delta(0)/kT_c \equiv 1.76$ (e.g., Fig. 2.6 of Ref. 11). These points greatly simplify the physics from a theoretical standpoint.
- (2) Because it is an amorphous alloy, the pinning is truly negligible under a wide range of conditions of j , B , and T (the mean-free-path between defects $l \approx 0.3$ nm is much less than the coherence length $\xi(0) \approx 5.2$ nm).
- (3) The high static disorder diminishes the relative contribution of temperature dependent electron-phonon scattering so that the normal-state resistivity $\rho_n(T) \simeq \text{const}$ over the temperature range of interest (ρ_n changes by less than 1% between 6.5K and 40K).
- (4) The high demagnetization of a film in transverse magnetizing field ensures, for $H \gg H_{c1}$ (where H_{c1} is the lower critical magnetizing field) a nearly homogeneous magnetic field B inside the sample with only a slight modulation at vortex positions. These facts make it an ideal system to obtain a clean first order understanding of the intrinsic dynamics of moving vortices.

II. EXPERIMENTAL TECHNIQUES

Films of thickness $t = 50$ nm were sputtered onto silicon substrates with 200 nm thick oxide layers from a $\text{Mo}_{0.79}\text{Ge}_{0.21}$ alloy target. The deposition system had a base pressure of 2×10^{-7} Torr and the argon gas working pressure was maintained at 3 mTorr during the sputtering. The growth rate was 0.15 nm/s. The samples were patterned into bridges of length $l = 102 \mu\text{m}$ and

width $w = 6 \mu\text{m}$ using photolithography and argon ion milling. Three samples are included in this study: Sample A with a transition temperature of $T_c=5.56$ K, sample B with $T_c=5.41$ K, and sample C with $T_c=5.15$ K. Their respective normal-state resistances (just above T_c) and upper-critical-field slopes were: $R_n = 555, 555, \text{ and } 630 \Omega$ and $H'_{c2} = dH_{c2}/dT|_{T_c} = -3.125, -3.125, \text{ and } -2.0 \text{ T/K}$.

Electrical resistivity measurements were made using the standard DC four-probe method and carried out in a pulsed-tube closed-cycle refrigerator inside a water cooled copper electromagnet.

III. THEORY

On the theoretical front, we could not find any work in the literature that treats flux flow under all general conditions of T and B —all theories are restricted in one way or another (e.g., T close to T_c , B close to H_{c2} , gapless case, etc.). Nevertheless, perhaps the most complete microscopic treatment of this phenomenon, which is unrestricted in its B/H_{c2} range, is that due to Larkin and Ovchinnikov (LO). That result and its theoretical underpinnings are well described in their own book chapter⁴ as well as in the book by Kopnin¹². The resulting expression can be written as:

$$\sigma_f = \sigma_n + \frac{\sigma_n}{(1-t)^{1/2}} \frac{H_{c2}}{B} \tilde{f}(B/H_{c2}). \quad (1)$$

Non-linearities that occur at higher values of B due to magnetic pair breaking and other mechanisms are included in the $\tilde{f}(B/H_{c2})$ function, which is given as Table 1 in their book chapter⁴. We found that this function can be well approximated by:

$$\begin{aligned} \tilde{f}(x) &= A_0 + A_1 e^{-x/t_1} + A_2 e^{-x/t_2} + A_3 e^{-x/t_3} \quad (\text{for } x < 0.5) \\ &= (1-x)^{3/2} [0.43 + 0.69(1-x)] \quad (\text{for } x > 0.5) \end{aligned}$$

with $A_0 = -0.05856$, $A_1 = 1.24535$, $A_2 = 0.8125$, $A_3 = 2.04068$, $t_1 = 0.00599$, $t_2 = 0.08961$, $t_3 = 0.27549$.

As an alternative to the formal LO theory, we will also analyze the data using the following simple heuristic model: For a film in a perpendicular magnetic field in the range $H_{c1} \ll B \ll H_{c2}$, the vortex cores are well separated but B is fairly spatially homogeneous with $B \simeq H$. In this case changing B only changes the areal number density of vortices and the free-flux-flow resistivity ρ_f must necessarily be proportional to B . Thus for this low B range, all theories of flux flow predict the form:

$$\rho_f = \nu \rho_n B 2\pi \xi^2 / \Phi_0 = \nu \rho_n B / H_{c2} \quad (2)$$

with a prefactor $\nu \sim 1$. We expect ν to possibly have some temperature dependence (which will be determined by the experiment). In this low B regime and for our temperature range of interest, which is $t = T/T_{c0} > 0.6$ (where T_{c0} is the transition temperature in zero B), H_{c2}

and ξ are well represented by

$$\frac{\Phi_0}{2\pi \xi^2(T)} = H_{c2}(T) = H'_{c2}[T - T_{c0}], \quad (3)$$

where H'_{c2} is the upper-critical-field slope $dH_{c2}(T)/dT$ at T_{c0} .

As B is increased beyond the above low-field regime, its pair breaking action will suppress the order parameter and cause the coherence length and vortex cores to expand¹⁹. We handle this additional B dependence by replacing T_{c0} in the the R.H.S. of Eq. 3 by the field suppressed transition temperature $T_{c2}(B) = T_{c0} + B \cdot H'_{c2}$. Eq. 2 thus becomes $\rho_f = 1/\sigma_f = (\nu \rho_n B) / (H'_{c2} \cdot [T - T_{c0} + B/H'_{c2}])$. (We consider the usual case for which the Hall angle $\theta_H \ll 1$, so that the flux flow conductivity $\sigma_f \simeq 1/\rho_f$.) To interpolate properly to the normal state we add the normal conductivity $\sigma_n = 1/\rho_n$ to the previous σ_f . This leads to the following heuristic expression for σ_f

$$\sigma_f = \sigma_n + \sigma_n \left(\frac{H'_{c2}[T - T_{c0}] - B}{\nu B} \right) \quad (4)$$

that should work for a wide range of T and B . Essentially it is the Bardeen-Stephen relationship modified to include magnetic pair breaking. Since σ_n , H_{c2} , and T_{c0} are directly measurable quantities, there is only the single adjustable parameter of $\nu \sim 1$. Eq. 4 causes ρ_f to have a stronger-than-linear (concave upwards curvature) B dependence. For clean superconductors, an opposite effect has been predicted by Kogan and Zhelezina (KZ)¹³ whereby the vortex cores shrink with increasing B leading to a weaker-than-linear (convex curvature). That regime has been seen in ultra clean single crystals of $V_3\text{Si}$ and $\text{LuNi}_2\text{B}_2\text{C}$ by Gapud et al.⁷.

IV. DATA AND ANALYSIS

Fig. 1 shows the mixed-state transport responses for samples A and B at two different temperatures. Panel (a) shows R vs I curves and panel (b) shows V vs I curves; both graphs are on linear-linear axes. As can be seen the chordal resistance $R = V/I$ is constant even at current densities that are several orders of magnitude below the pair breaking value j_d ; for example, at $I = 10 \mu\text{A}$, $j = 3.3 \times 10^3 \text{ A/cm}^2$ whereas¹⁵ $j_d(0) \approx 0.009 \times \sqrt{H_{c2}(0)/\lambda^2(0)} \sim 3 \times 10^7 \text{ A/cm}^2$ (a compilation of parameters for MoGe is given in reference 16). Furthermore, the behavior is completely reversible and there is no hysteresis with respect to cycling of the sample current, temperature or magnetic field. To our knowledge this is the cleanest demonstration of Ohmic behavior in the free flux flow regime.

Fig. 2(a) shows for sample A the free-flux-flow resistances as measured above (every point is exactly Ohmic and on a constant R plateau) plotted against the magnetic field. The different curves correspond to different

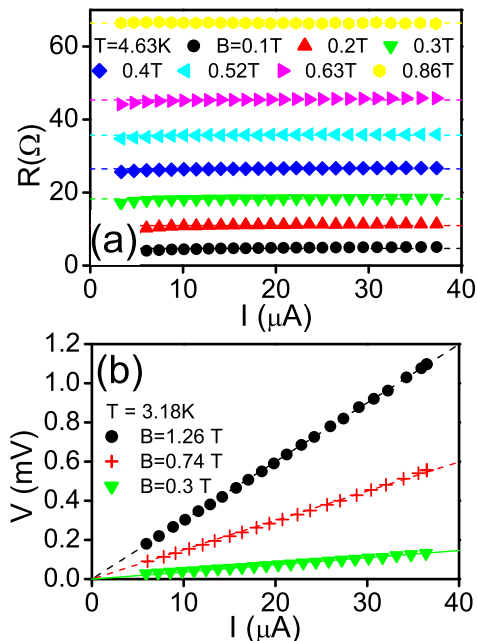


FIG. 1: (a) R vs I curves for sample A. The horizontal lines are least-squares fits to the data. (b) V vs I curves for sample B. The lines are least-squares fits to the data extrapolating to the origin.

temperatures as indicated. At low B the response is linear and at higher B it becomes more strongly varying causing the upward concave curvature. The solid lines correspond to the LO theory (Eq. 1). As can be seen the overall agreement is not good—the theory predicts too strong a B dependence and has excessive curvature. Fig. 2(b) shows the same data fitted to our heuristic model. The overall shapes of the curves are in much better agreement with the measured data. For each curve we take ν as a fitting parameter so that the dependence $\nu(T)$ can be determined. Fig. 3 is a similar set of LO and heuristic fits to data for another sample, showing the same characteristic behavior. The values of $\nu(T)$ obtained for samples A and B—corresponding to the fits in Fig. 2(b) and Fig. 3(b)—are shown in Fig. 4 as the circles and squares respectively. Also shown is a set of $\nu(T)$ values for a third sample, the triangles corresponding to sample C, measured at three temperatures. As can be seen, the observed $\nu(T)$ is relatively flat with respect to temperature with a value of $0.316 \pm 0.042 \approx 1/3$ averaged over all three MoGe samples.

Fig. 5 shows the resistive transitions in various magnetic fields to see how well different theories describe the behavior as one approaches T_c . From panels (a) and (b) it can be seen that our heuristic model works much better than the LO theory. Since this data is in the vicinity of T_c , it is also of interest to see how well the TDGL (time dependent Ginzburg-Landau) theory works here (even though it is strictly speaking valid only for gapless superconductors). Panel (c) shows fits to the

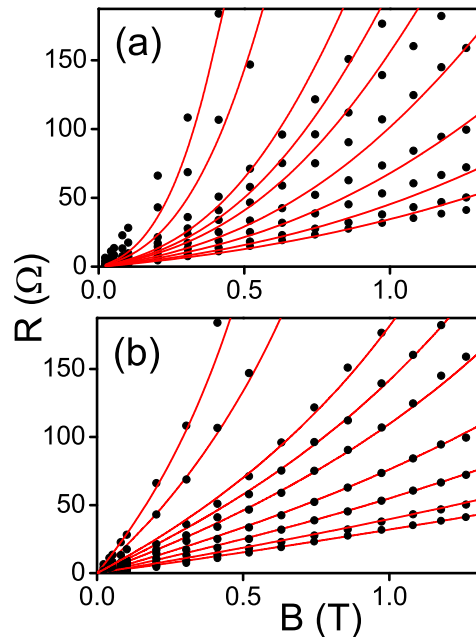


FIG. 2: Resistance versus magnetic field data (symbols) for sample A at temperatures (bottom to top): $T = 3.25, 3.74, 4.24, 4.56, 4.79, 4.90, 5.00, 5.21, 5.31\text{K}$. (a) Fits to LO theory (Eq. 1) with $H_{c2}(T)$ given by $H_{c2}(T) = H'_{c2}[T - T_c]$ and the measured value $H'_{c2} = -3.125\text{T}$. (b) Fits to the heuristic model (Eq. 4) using ν as a fitting parameter for each curve. The resulting values of ν are shown in Fig. 4.

same data using the TDGL based theory of Troy and Dorsey⁵; that theory can be cast into a form similar to Eq. 4 with $\nu(T) = \frac{32\sigma_n\mu_0\beta_A\lambda^2(0)kT_c}{h(1+t)(1+t^2)} \approx \frac{1}{(1+t)(1+t^2)}$. The TDGL theory works better than LO, but still not as well as the heuristic model. The formal theories have extra B and/or T dependence which is not followed by the observed phenomenon—nature is simpler and follows the basic Bardeen-Stephen like behavior (with a T and B independent prefactor of $\nu \sim 1/3$) modified to include magnetic pair breaking.

We looked through the literature for other data that might be at least approximately in the free flux flow regime to test the validity of the heuristic model for other materials. Fig. 6(a) shows a plot of normalized R versus normalized B data for amorphous Nb_3Ge films taken from Berghuis et al.¹⁰ and Fig. 6(b) shows R versus T plots for $\text{Bi}_2\text{Sr}_2\text{CaCu}_2\text{O}_8$ crystals taken from Chen et al.¹⁸. Notwithstanding the fact that the data correspond to differential resistance or have not been checked for Ohmic behavior, these are both systems well known for their very low pinning characteristics and therefore we expect that the data should lie at least approximately in the free flux flow regime. As can be seen, the solid lines, corresponding to fits to our heuristic model, are in good agreement with the trends of the measured data. For the Nb_3Ge data, the fit yields a ν value of 0.27, comparable to what we observe in MoGe; this datum is shown

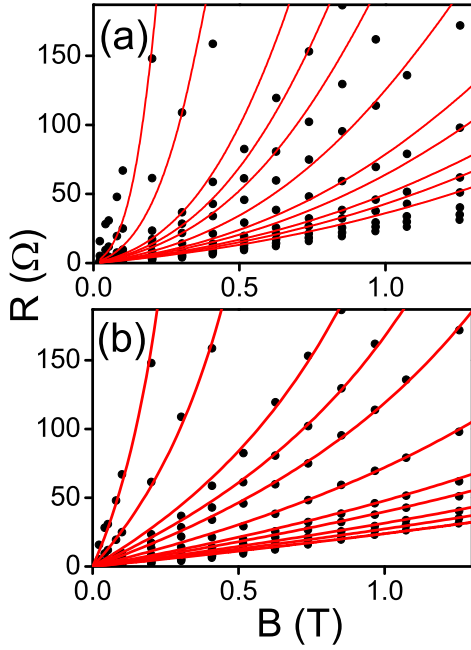


FIG. 3: Resistance versus magnetic field data (symbols) for sample B at temperatures (bottom to top): $T = 3.17, 3.48, 3.71, 4.01, 4.21, 4.53, 4.77, 4.88, 4.98, 5.19, 5.30$ K. (a) Fits to LO theory (Eq. 1) with $H'_{c2}(T)$ given by $H'_{c2}(T) = H'_{c2}[T - T_{c0}]$ and the measured value $H'_{c2} = -3.125$ T. (b) Fits to the heuristic model (Eq. 4) using ν as a fitting parameter for each curve. The resulting values of ν are shown in Fig. 4.

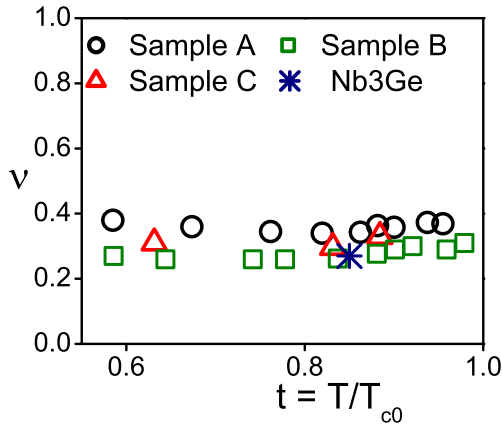


FIG. 4: Experimentally deduced parameter ν (of Eq. 4) and its variation with temperature for the three MoGe samples A, B, and C. The asterisk shows a datum corresponding to the Nb_3Ge sample of reference 10.

as an asterisk on Fig. 4. For the $Bi_2Sr_2CaCu_2O_8$ data, a different ν value is required for each field; however, all curves were fitted using the published¹⁷ value of $H'_{c2} = -0.75$ T/K rather making this an adjustable parameter. In their paper, Chen et al. fit the curves using a different value of H'_{c2} for each B .

As long as the transport response follows the heuris-

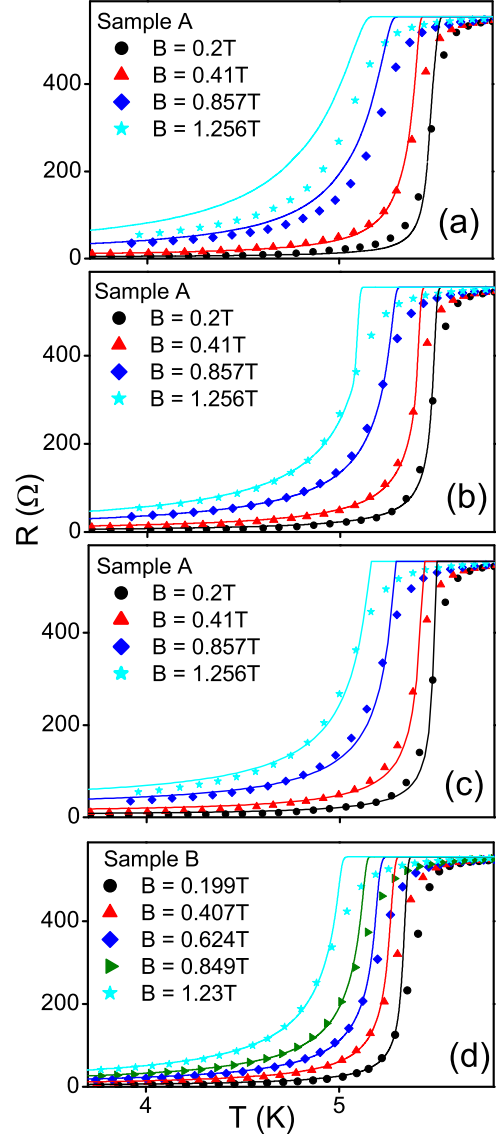


FIG. 5: Resistive transitions in magnetic fields. Panels (a), (b), and (c) show fits to the same set of data on sample A using LO, heuristic-model, and TDGL theories. Panel (d) shows data for sample B with heuristic-model fits.

tic model, Eq. 4 suggests the following way to linearize and collapse conductance-versus-temperature data at the transition: we define a “normalized excess conductivity” $\sigma' = (\sigma - \sigma_n)B/\sigma_n$ and plot this against a “shifted temperature” $T' = T - B/H'_{c2}$. Such plots are shown in Fig. 7 for the three samples. This scheme provides an unambiguous method for determining H'_{c2} since the choice of this parameter causes the curves to collapse over the entire resistance range and not just at some arbitrary criterion such as $R_n/2$ or the onset²⁰. The slope of the collapsed curves equals H'_{c2}/ν and the x -intercept equals T_{c0} .

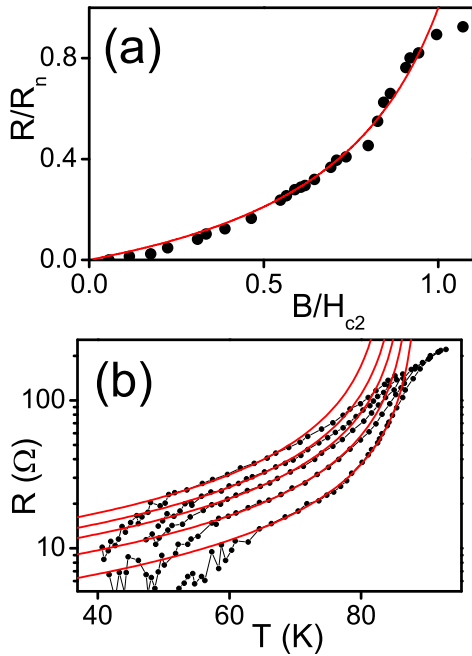


FIG. 6: Heuristic model (Eq. 4) fits (lines) to flux flow data (symbols) in other materials. (a) Normalized resistance versus normalized field for amorphous Nb_3Ge films from Berghuis *et al.*¹⁰. $T = 2.49$ K and $T_c = 2.93$ K. (b) R vs T curves for $Bi_2Sr_2CaCu_2O_8$ from Chen *et al.*¹⁸. From bottom to top, $B = 1, 2, 3, 4,$ and 5.5 T; correspondingly $\nu = 0.9, 0.64, 0.54, 0.47,$ and 0.39 . $T_c = 89$ K and $H'_{c2} = -0.75$ T/K.

V. CONCLUSIONS

Free flux flow is the most primitive regime of transport in the mixed state; however, its theoretical description is anything but simple since it entails nonequilibrium processes whose microscopic treatment is complex and involved. What is the observed reality and what are the subtle alterations to the dynamics as the vortices get closer: Is there an expansion of the vortex—as LO, TDGL, and our heuristic model predict—or is there shrinkage due to cancellation of circulating currents as per the KZ mechanism? Normally it is difficult to address such questions because of the gross alteration to the dynamics caused by pinning and other complications (dissociation into pancakes due to a layered structure, exotic gap symmetries, melting/entanglement due to high temperatures, etc.). The present experiment has observed the cleanest FFF behavior in one of the simplest and most model of superconductors (unpinned, isotropic, low-temperature, weak-coupling BCS, etc.). This allows us a first close look at the true intrinsic transport char-

acteristics of the free flux flow regime. We find that the theory by Larkin and Ovchinnikov does not give a correct account of the observed behavior, predicting excessively strong T and B dependencies. Instead, nature appears to be much simpler and can be well described by a heuristic model that is along the lines of the Bardeen-Stephen

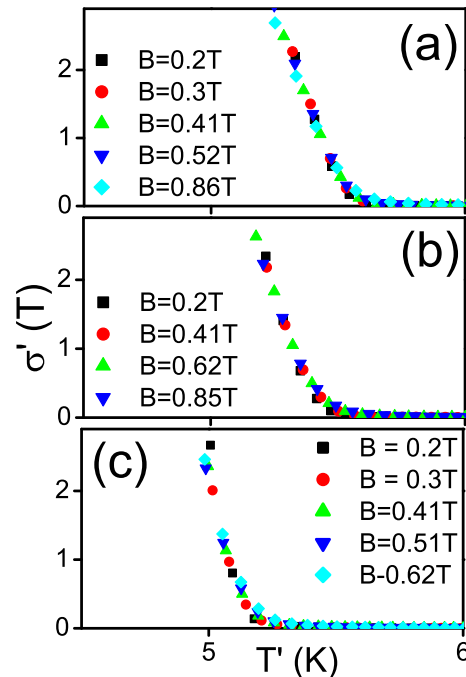


FIG. 7: Plots of the normalized excess conductivity $\sigma' = (\sigma - \sigma_n)B/\sigma_n$, versus the shifted temperature $T' = T - B/H'_{c2}$. Panels (a), (b), and (c) correspond to the samples A, B, and C. For each sample, all data collapse onto a universal linear curve whose slope equals H'_{c2}/ν and the x-intercept equals T_{c0} .

model with a straightforward modification to include magnetic pair breaking.

VI. ACKNOWLEDGEMENTS

The authors gratefully acknowledge useful discussions with James M. Knight, Boris I. Ivlev, Alexander V. Gurevich, Vladimir G. Kogan, Lev Bulaevski, David K. Christen, and Ernst Helmut Brandt. This work was supported by the U. S. Department of Energy through grant number DE-FG02-99ER45763. The sample fabrication work at Northern Illinois University was supported by the U.S. Department of Energy through grant number DE-FG02-06ER46334.

* Corresponding author email: kunchur@sc.edu;
URL: <http://www.physics.sc.edu/kunchur>

¹ J. Bardeen and M. J. Stephen, Phys. Rev. **140**, A1197 (1965).

- ² J. R. Clem, Phys. Rev. Lett. **20**, 735 (1968).
- ³ M. Tinkham, Phys. Rev. Lett. **13**, 804 (1964).
- ⁴ A. I. Larkin and Yu. N. Ovchinnikov, in *Nonequilibrium Superconductivity*, D. N. Langenberg and A. I. Larkin, eds. (Elsevier, Amsterdam, 1986), Ch. 11.
- ⁵ R. J. Troy and A. T. Dorsey, Phys. Rev. B **47**, 2715 (1993).
- ⁶ M. N. Kunchur, D. K. Christen, and J. M. Phillips, Phys. Rev. Lett. **70**, 998 (1993).
- ⁷ A. A. Gapud et al., Phys. Rev. B **80**, 134524 (2009).
- ⁸ K. Das Gupta, S. S. Soman, N. Chandrasekhar, Physica C **388–389**, 771 (2003).
- ⁹ F. Lefloch, C. Hoffmann, and O. Demolliens, Physica C **319**, 258 (1999).
- ¹⁰ P. Berghuis, A. L. F. van der Slot, and P. H. Kes, Phys. Rev. Lett. **65**, 2583 (1990).
- ¹¹ J. M. Graybeal, Ph.D. thesis, Stanford University, 1985.
- ¹² *Theory of Nonequilibrium Superconductivity* by N. B. Kopnin, The International Series of Monographs on Physics (by Oxford University Press, USA, 2009)
- ¹³ V. G. Kogan and N. V. Zhelezina, Phys. Rev. B **71**, 134505 (2005).
- ¹⁴ N. R. Werthamer, E. Helfand, and P. C. Hohenberg, Phys. Rev. **147**, 295 (1966)
- ¹⁵ M. N. Kunchur, J. Phys.: Condens. Matter **16**, R1183-R1204 (2004); and references therein.
- ¹⁶ W. L. Carter, Ph.D. thesis, Stanford University, 1983.
- ¹⁷ T. T. M. Palstra, B. Batlogg, L. F. Schneemeyer, R. B. van Dover, J. V. Waszczak, Phys. Rev. B **38**, 5102 (1988).
- ¹⁸ W. Chen, J. P. Franck, and J. Jung, Physica C **341–348**, 1195 (2000).
- ¹⁹ The estimated $H_{c2}(0) \approx 0.7 T_c H'_{c2} \approx 11$ T (from the measured H'_{c2} and WHH¹⁴ extrapolation) is of the order of the Pauli paramagnetic limit of $H_p = 1.84 T_c \approx 10$ T. Furthermore, the spin-orbit scattering rate $\tau_{so}^{-1} \sim 7.7 \times 10^{11} s^{-1}$ (as per Ref. 11) is not high enough to satisfy the condition $\tau_{so}^{-1} m / eB \gg 1$ to be in the random-walk averaging regime. Hence the T_c suppression by B should be linear as indeed observed.
- ²⁰ If pinning is severe, then the transitions are nearly vertical and parallel at all B values and then no ambiguity arises from the criterion used to define the $H_{c2}(T)$ boundary.